

# Improving Grip Stability Using Passive Compliant Microspine Arrays for Soft Robots in Unstructured Terrain

Lauren Ervin, Harish Bezawada, and Vishesh Vikas<sup>1</sup>

**Abstract**—Microspine grippers are small spines commonly found on insect legs that reinforce surface interaction by engaging with asperities to increase shear force and traction. An array of such microspines, when integrated into the limbs or undercarriage of a robot, can provide the ability to maneuver uneven terrains, traverse inclines, and even climb walls. Conformability and adaptability of soft robots makes them ideal candidates for these applications involving traversal of complex, unstructured terrains. However, there remains a real-life realization gap for soft locomotors pertaining to their transition from controlled lab environment to the field by improving grip stability through effective integration of microspines. We propose a passive, compliant microspine stacked array design to enhance the locomotion capabilities of mobile soft robots, in our case, ones that are motor tendon actuated. We offer a standardized microspine array integration method with effective soft-compliant stiffness integration, and reduced complexity resulting from a single actuator passively controlling them. The presented design utilizes a two-row, stacked microspine array configuration that offers additional gripping capabilities on extremely steep/irregular surfaces from the top row while not hindering the effectiveness of the more frequently active bottom row. We explore different configurations of the microspine array to account for changing surface topologies and enable independent, adaptable gripping of asperities per microspine. Field test experiments are conducted on various rough surfaces including concrete, brick, compact sand, and tree roots with three robots consisting of a baseline without microspines compared against two robots with different combinations of microspine arrays. Tracking results indicate that the inclusion of microspine arrays increases planar displacement on average by 15 and 8 times over the baseline with the two microspine designs respectively, improves locomotion repeatability, and, critically, consistently increases terrain traversability.

## I. INTRODUCTION

In nature, animals resist slipping and falling by increasing interaction with surfaces in a number of ways. Snakes maintain a large surface area in contact with the ground to increase the amount of propulsive force aiding in locomotion. Snake inspired robots are developed with textured skins for increased traction [1], [2]. However, the efficacy is unknown for limbed robots equipped with these skins and will require additional coordination. Geckos utilize van

der Waals interactions to provide an adhesive force against surfaces. Attaching gecko inspired, synthetic adhesives to extremities of robots is an attractive option due to the range of surfaces the robots can adhere to [3]–[7]. These directional adhesion mechanisms are sensitive to wear and tear and require periodic cleaning for reliable adhesion. Insects such as caterpillars and cockroaches are able to climb vertical surfaces with small spines attached to their legs. These microspine grippers increase shear force and traction by engaging with surface asperities. They do not penetrate surfaces, but rather reinforce surface interaction by gripping onto jagged, microscopic edges. Biological studies have looked at the relationship between microspine arrays and surface interaction, comparing the efficacy on different smooth and rough surfaces [8]. The outcome from these studies encourage the creation of synthetic microspine arrays to enable maneuverability of uneven terrains, traversability of inclines, and climbing walls [9]–[19]. These arrays can become very complicated, and there exists a trade-off between design complexity and surface adaptability for many of these robots as shown in Fig. 1.

Climbing and crawling rigid robots developed in the past decade employ similar methods to combat slipping along vertical walls [18], [20]–[23]. JPL’s LEMUR IIB, a four-limbed robot, features multiple grippers, each equipped with at least 250 microspines capable of adhering to both convex and concave surfaces. Each microspine is suspended with a steel hook, allowing it to stretch and move relative to its neighbors to find suitable surfaces to grip. This enables the robot to climb vertically and traverse on cave ceilings. The shear forces from the microspines integrated in the gripper gives the ability to support heavy loads [24]. These grippers possess the necessary traction to navigate micro-gravity environments, such as asteroids, comets, and small moons, where conventional ground pressure is lacking [25]. Microspines latch into small asperities on a rock’s surface such as pits, cracks, slopes, or any kind of topography that will snag a hook. Success of an individual spine catching is dependent on surface roughness, surface geometry, and asperity distribution [26].

Integrating microspines into Soft Robots (SoRos) is an attractive option due to their adaptability and conformability to changing surface topologies, highlighted in Fig. 2. The continuum nature and impact resistance of soft materials passively allow SoRos additional flexibility and more effective interaction with complex and non-uniform surfaces. However, SoRos lack grip stability, contributing to them historically struggling with efficient locomotion as well as

<sup>\*</sup>This work was supported in part by NSF #1830432. The material contained in this document is based upon work supported in part by a National Aeronautics and Space Administration (NASA) grant or cooperative agreement. Any opinions, findings, conclusions, or recommendations expressed in this material are those of the authors and do not necessarily reflect the views of NASA. This work was supported through a NASA grant awarded to the Alabama/NASA Space Grant Consortium.

<sup>1</sup>Lauren Ervin, Harish Bezawada, and Vishesh Vikas are with the Agile Robotics Lab, University of Alabama, Tuscaloosa, AL 35487, USA {lefaris, hbezawada}@crimson.ua.edu, vvikas@ua.edu

locomoting over unstructured terrain. Because of this, SoRo designs that can traverse outside and perform real tasks outside of a lab setting are under-researched. Utilizing microspines has the potential to improve traction, increase grip stability, and provide the ability to reliably maneuver real-world terrains. One of the main design challenges pertains to integrating a soft, low stiffness body with hard, high stiffness microspines. A two segment, wriggling SoRo avoids this challenge by adhering an array of dual material, “soft microspines” made of rubber along the ventral of the body to successfully increase anisotropic friction [27]. A starfish inspired SoRo implements a similar technique by including soft, tube feet reminiscent of microspines along the entire underside of the five-limbed robot. Magnetization of the tube feet allows omnidirectional movement and reduces the motion resistance from the ground, enhancing the adaptability of the SoRo on different surfaces [28]. Embedding hard objects in soft materials through intelligent mechanical design is necessary to take advantage of the benefits of hard spines without hindering the soft deformable properties. A soft inchworm design attaches an array of microspines to either foot of the inchworm using adhesive bonding technology [29]. However, deeply irregular surfaces remain difficult if not impossible to overcome due to the uniform distribution of the microspines and integration technique that restricts the usage to surfaces with regular, fine asperities. This shows the need for compliance and independent movement per microspine to increase surface geometry traversability.

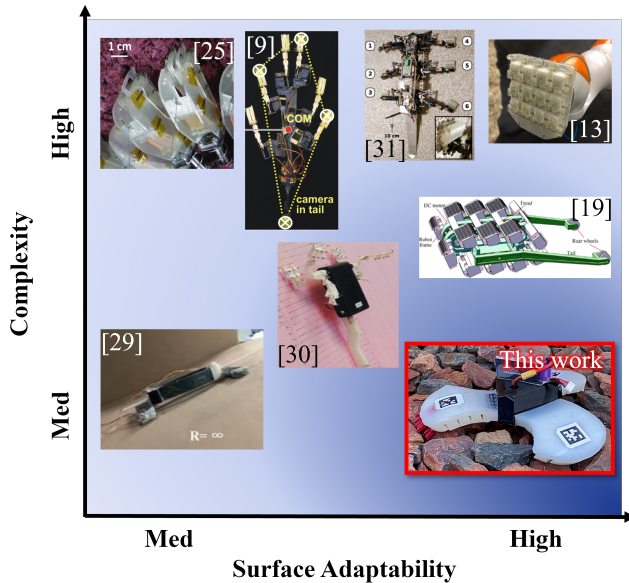


Fig. 1: Surface adaptability vs. design complexity with various microspine robots [9], [13], [19], [25], [29]–[31] compared against one of the presented designs, 1ML.

*Contributions.* We aim to bridge the realization gap by attaching microspine technology onto the tips of soft Motor Tendon Actuated (MTA) limbs, vastly improving the grip stability and types of traversable terrain of mobile SoRos. We



Fig. 2: Conformable nature of soft limbs enable traversal over large tree root present on forest floor surface.

propose an elegant, single-material design with intelligent soft-compliant integration that reduces complexity by using a single actuator to passively control an entire array fixed to the end of a soft limb. In this research, we (1) propose a compliant mechanism, two-row stacked microspine array design that improves grip stability and increases traversable surface topologies of mobile SoRos; (2) identify critical design parameters that improve locomotion capabilities while reducing complexity by controlling an entire microspine array with only a single actuator through intelligent soft-compliant integration; (3) investigate the grip stability and repeatability of a baseline SoRo compared against two different microspine array configurations on uniform concrete, partially uniform brick, granular compact sand, and non-uniform tree roots; and (4) analyze tracking results that indicate the inclusion of compliant microspine arrays in SoRos increases planar displacement on all surfaces through enhanced surface engagement resulting in capabilities to traverse complex, unstructured environments.

*Paper Organization.* The next section explores critical design parameters of the compliant mechanism microspine array and the SoRo prototype. The third section discusses the three experimental prototypes, experimental setup, and pose estimation algorithm. The fourth section highlights the results, validating the microspine array design. The fifth section concludes the paper and discusses the future work.

## II. MICROSPINE ARRAY AND ROBOT DESIGNS

There are several design parameters that impact the effectiveness of microspines. The critical ones include (1) adding compliance to individual microspines and the angle at which the microspines interact with a surface, (2) the array configuration and (3) effective integration with the robot body. Even with an optimal design, the microspine array will not be effective on every surface. The aspects that are out of the hands of the designer, but also highly impact surface engagement, include surface roughness, distribution of asperities, and size of asperities.

### A. Compliant Mechanism Microspine Design

The single-material mechanism, shown in Fig. 3, allows compliance with an exposed joint while simplifying the

fabrication process over previous microspine designs. The compliant mechanism is fabricated with an FDM 3D printer and TPU with 95A Shore hardness. Halfway through the additive manufacturing process, the print is paused. The microspine is inserted into a channel left in the middle of the mechanism, highlighted in Fig. 3c), and the print is resumed. Once finished, the angle of the bare microspine can be modified for different surface topologies while the body remains secure in the mechanism. The angle of surface interaction,  $\alpha$ , was fixed at roughly  $45^\circ$  during testing.

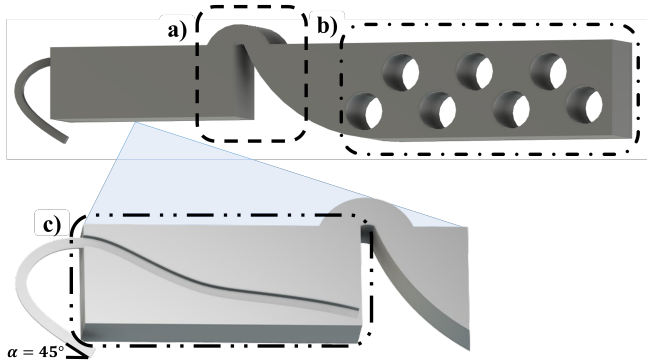


Fig. 3: Compliant mechanism design. a) A hinge joint enables passive compliance. b) Holes embedded on the righthand side of the mechanism allow anchoring into the silicone limb. c) A microspine is inserted in a center channel matching the spine topology set halfway into the mechanism.

### B. Microspine Array Configuration

The array configuration ensures multiple microspines remain active on various complex surfaces. We propose a two-row, stacked array configuration consisting of ten microspines with four on the top row and six on the bottom. The microspines on the bottom row are commonly active on more uniform terrain. The top row can become active on steep/highly irregular surfaces without hindering the movement of the bottom row of microspines. The critical parameter when designing the array configuration is ensuring adequate surface interaction and gripping regardless of topology. Crucially, not all microspines need to interact with a surface for the microspine array to be effective, shown in Fig. 4. This is a byproduct of the passive nature and built-in redundancy of the system.

### C. Effective Soft-Compliant Integration Through Anchoring

The soft-compliant integration reduces design complexity by allowing each microspine to passively move independent of one another with a single actuator controlling the entire array configuration. To achieve this, a mold is created with channels for each microspine compliant mechanism to attach to the tip of a SoRo limb. The SoRo prototype used for experimentation is cast out of DragonSkin™ silicone rubber using a custom mold, shown in Fig. 5. Therefore, a modified limb mold is used for integrating the microspine array in a consistent, standardized manner. Half of the compliant

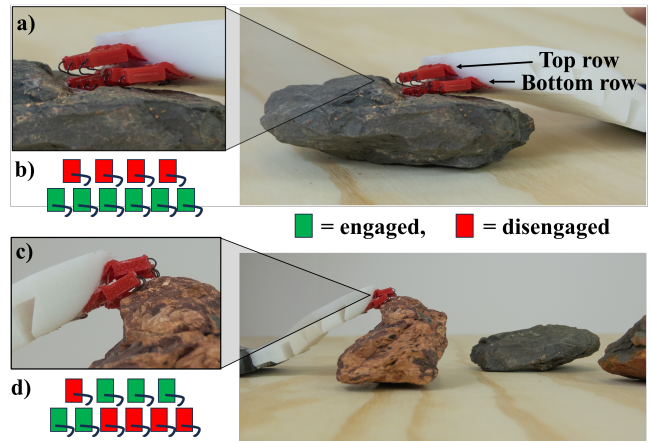


Fig. 4: Two-row, stacked array configuration. a) Close-up of the microspines gripping onto a non-uniform rock. b) This diagram highlights which microspines are interacting with the surface. On this rock, all 6 of the microspines on the bottom row are active. c) Close-up of the microspines gripping onto a steeper rock. d) On this rock, 2 of the bottom row and 3 of the top row microspines are active.

mechanism contains holes that mechanically anchor it into the silicone limb, highlighted in Fig. 3b), preventing it from being freely pulled out of the limb during microspine gripping. This anchoring method is essential for ensuring the microspine does not come loose over time. The remaining, exposed half of the mechanism contains the microspine.

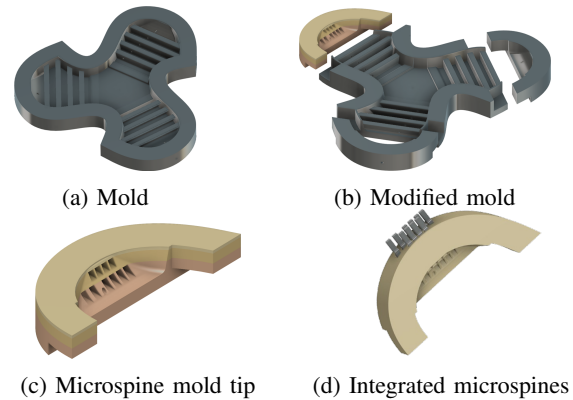


Fig. 5: Modular ends of the mold enable soft-rigid integration. a) A baseline robot mold. b) A modified mold that allows different configurations of microspine arrays per limb. c) Microspine compatible end mold with holes for a two-row stacked microspine array configuration. d) End mold with integrated microspine mechanisms and ready for casting.

### D. Soft Robot Design

A tetherless, three limb MTA SoRo with on-board power and processing with AprilTags on each limb is used as the experimental prototype. The components of the physical robot are shown in Fig. 6. Outward trapezoid cavities are introduced on the underside of each limb to provide optimal

stiffness and curling ability. This allows the robot to lift the limb and electronic payload. The use of MTA for body deformation enables reliable and efficient limb actuation. The reader may refer to [32] for more details.

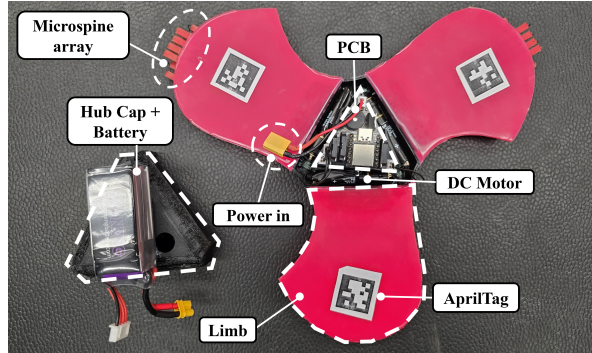


Fig. 6: The externally powered three-limb SoRo contains soft material limbs and a flexible, central hub that houses DC motors and a custom-designed PCB. The three AprilTags on the limbs help with pose tracking during experiments.

### III. EXPERIMENTATION

#### A. Experimental Prototypes

The baseline experimental prototype with zero microspine limbs, OML, is a three-limb MTA SoRo coming from a previous work [33]. We compare the baseline against the addition of two different microspine configurations. The first SoRo equipped with a microspine array, 1ML, has them affixed to one limb that acts as the leader. The last SoRo, 2ML, contains microspine arrays equipped on two limbs with these acting as dual leaders. In all microspine configurations, the microspines face opposite the intended direction of movement. CAD models of the three prototypes are shown in Fig. 7.

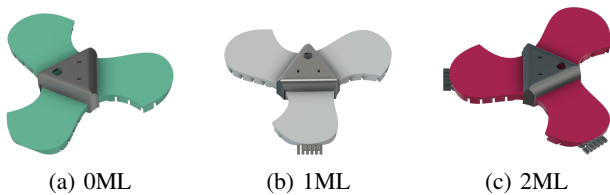


Fig. 7: The three different microspine configurations explored in the experiments: a) a baseline aqua SoRo; b) a white SoRo with a total of 10 microspines configured in an array on one limb; c) a red SoRo with a total of 20 microspines configured in two arrays on two limbs.

A push-pull translation gait, Fig. 8, is used for the experiments. Here the gait sequence involves actuation of one limb followed by actuation of the two relaxed limbs. It is worth reminding the reader that this gait is not optimal for all four surfaces and three prototypes. In a previous work, translation and rotation gaits were discovered for four limb SoRos using an environment-centric framework [33]. The same methodology was used to generate an optimal

translation gait for the baseline three limb SoRo (OML) on a rubber mat. This gait was used on all surfaces for OML, 1ML, and 2ML for a fair comparison, but it is expected that much better performance is possible with an optimized gait found for each prototype and surface combination.

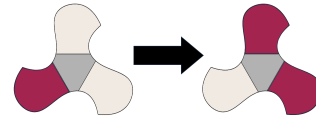


Fig. 8: Translation gait: one limb (in maroon) actuates while the other two relax, then the previously relaxed limbs actuate while the other relaxes. This is an optimal, 1.1s long gait for the baseline SoRo on a rubber mat [33].

#### B. Experimental Setup

The experiments are carried out with an overhead camera attached to a tripod next to the test area, shown in Fig. 9. Field tests are performed on four different surfaces. The starting pose, position and orientation, is same for each SoRo to ensure consistency. Tracking is performed with an AprilTag fixed to the end of each limb serving as fiducial markers. The average displacement per gait as well as overall displacement for each trial run is recorded.

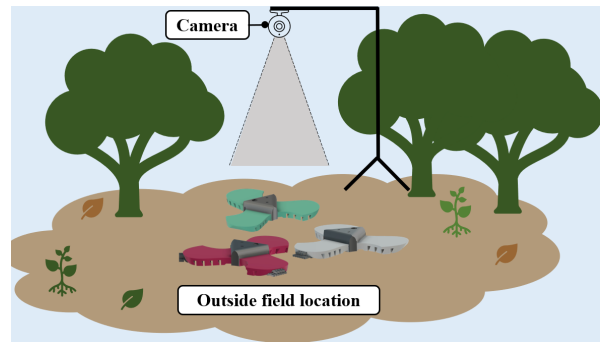


Fig. 9: Example of experimental setup for outside field locations in a forest with a dirt patch. The overhead camera is orthogonal to the ground and approximately 4' above the surface. Experiments took place with the three prototypes discussed previously: OML, 1ML and 2ML.

#### C. Field Experiments

The field experiments are tested on four rough surfaces around the University of Alabama campus. We look at uniform concrete, partially uniform brick, granular compact sand with pebbles, and a non-uniform forest floor containing leaf litter and large tree roots. Tests are conducted using the push-pull translation gait shown in Fig. 8. Three trials (60 gaits per trial) are performed for a particular configuration and surface with three prototypes and four surfaces, resulting in a total of 36 trials.

A 36h11 family AprilTag from the AprilTag visual fiducial system [34] is attached to each limb where they are readily visible while not hindering the movement. To compensate

for occlusion and easy access to the hub, three tags were used to find the robot's position. Each limb of a robot has a different tag attached which represents a number from 0 – 8. Before starting the tracking, the threshold parameters for different background environments are obtained. The tags are detected using an AprilTag detector library in Python. The tracking algorithm and data processing code is available at [github.com/AgileRoboticsLab/SoftRobotics-Microspines](https://github.com/AgileRoboticsLab/SoftRobotics-Microspines).

#### IV. RESULTS

The translation results of 0ML, 1ML, and 2ML are compared on 4 surfaces. Fig. 10 shows the average displacement and standard deviation of the 3 trials per prototype.

The concrete surface is level with a uniform distribution of asperities. Here, both 1ML and 2ML outperform 0ML in terms of displacement. In fact, 1ML had an average displacement of 39.63cm which is over 30 times as much as the 1.32cm that 0ML traveled. 2ML traveled 14.13cm, nearly 11 times as much as 0ML. 2ML had higher consistency across trials, having a standard deviation of 0.76 whereas 0ML's standard deviation was 0.83.

The partially uniform brick contains gaps in between bricks that can cause microspines to become stuck. This was observed to happen randomly across all trials. However, in every instance where this occurred, the microspine that was caught on 1ML or 2ML was able to wiggle free within a few seconds and continue moving. Even with these obstacles, both 1ML traveling 15cm and 2ML traveling 10.52cm had far greater average displacement than 0ML, roughly 25 times and 18 times more, respectively. This was the only surface where 0ML had the lowest standard deviation, and this is due to the microspine limbs on the other two robots randomly getting stuck when crossing over brick perimeters. Additionally, this surface resulted in the lowest overall movement of 0ML, with an average displacement of 0.59cm.

The granular, compact sand was not entirely level and various pebbles, holes, insects, and small sticks were scattered around the testing area. This surface was difficult to overcome for all three robots as the compact sand was covered in a loose, granular top layer that was easy to become partially submerged in. Due to this, the average displacement is far lower on this surface. The two microspine limbs on 2ML seemed to dig itself deeper, resulting in average displacement of only 0.46cm and the lowest standard deviation. 1ML still outperformed 0ML with over 3 times increased displacement, traveling 2.53cm compared to 0.82cm.

The forest floor surface was completely non-uniform with highly varying terrain. Specifically, the prototypes had to first overcome a large, 4" tall tree root and then move through leaves, acorns, and other tree debris. All SoRos were able to successfully traverse over the cylinder-like tree root due to the conformable nature of the soft limbs, highlighted in Fig. 2. However, only the 1ML and 2ML were able to navigate through the thick tree debris after making it over the large tree root; 0ML became stuck at the base of the tree root in each of its three trials. This is exhibited in the average displacement of 13.74cm for 0ML, 23.95cm for 1ML, and

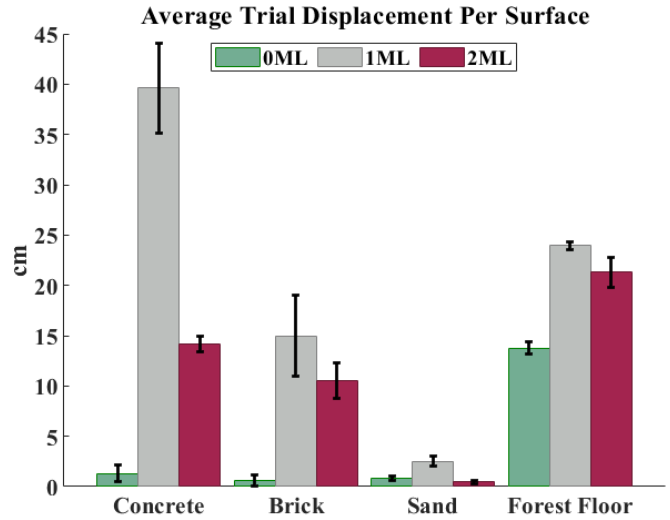


Fig. 10: The average displacement data per prototype and surface combination. The repeatability is shown in error bars.

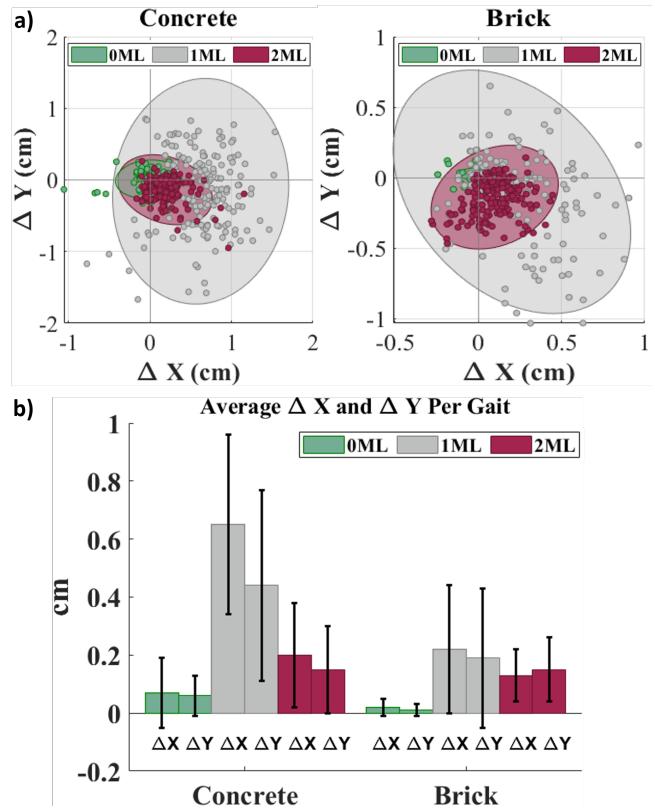


Fig. 11: Gait analysis. a) Every  $\Delta X$  and  $\Delta Y$  position per gait on concrete and brick. b) The average absolute  $\Delta X$  and  $\Delta Y$  displacement data per gait on concrete and brick.

21.32cm for 2ML. The forest floor was critical for testing as it was the most unstructured of the four experimental surfaces and showcases the benefits of the soft limbs paired with the added gripping stability of the microspine array.

For each of the 36 trials, the robots move for 60 gaits, resulting in a total of 2,160 gaits or 720 gaits per robot. Each

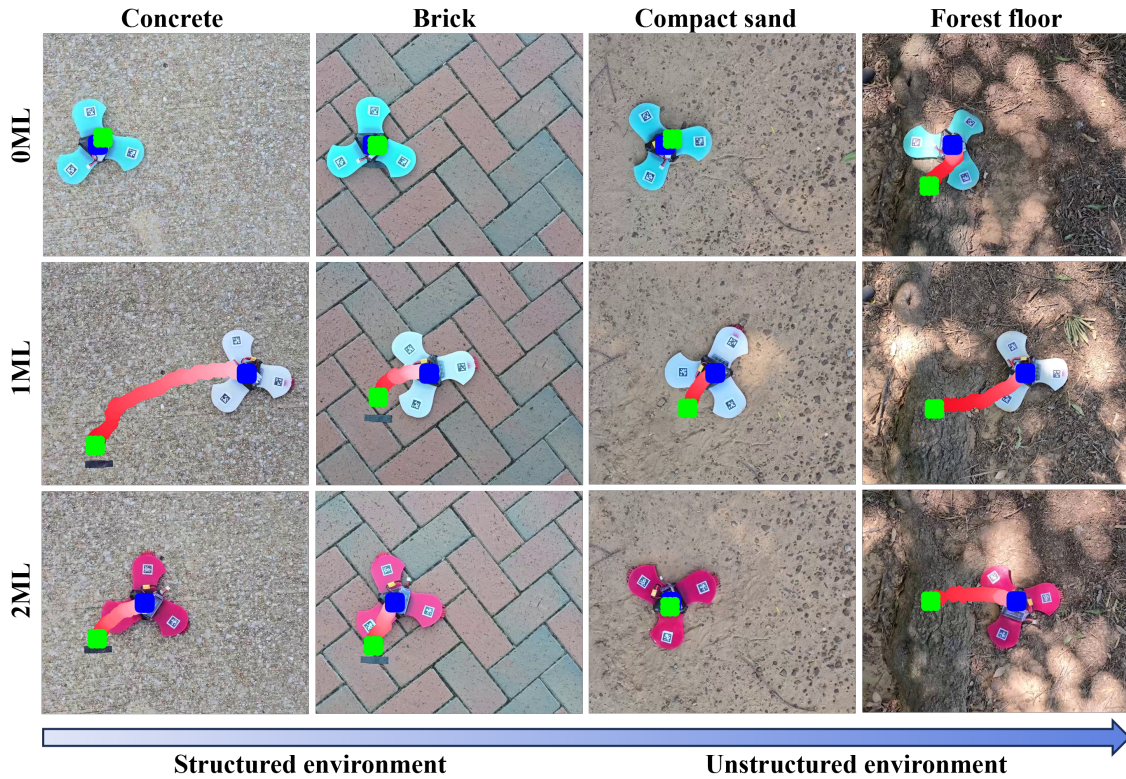


Fig. 12: Experimental results for 0ML, 1ML, and 2ML on concrete, brick, compact sand, and a forest floor. Rows represent the different surfaces increasing in unstructured nature with the three different prototypes distinguished by columns.

gait results in relative change in position in the robot coordinate system  $\Delta X, \Delta Y$ . The locomotion consistency can be analyzed by examining the 180 poses on a given surface per prototype, such as those shown in Fig. 11a). The average displacement per gait ( $\Delta X, \Delta Y$ ) as well as the standard deviation over all gaits per prototype/surface combination is visualized in Fig. 11b). We only analyze the uniform/partially uniform surfaces as the gait-to-gait movement is much less consistent due to non-uniformity and randomness for the other two surfaces. On concrete, the average gait displacement per gait of both 1ML (0.65cm, 0.44cm) and 2ML (0.20cm, 0.15cm) is greater than 0ML (0.07cm, 0.06cm). On brick, both 1ML (0.22cm, 0.19cm) and 2ML (0.13cm, 0.15cm) outperform 0ML (0.02cm, 0.01cm). The relative standard deviation (standard deviation/mean) for 1ML and 2ML is lower than that for 0ML, indicating greater grip stability through improved repeatability.

Examples of a single trial of each prototype row on each surface column is visualized in Fig. 12 with additional data in the accompanying video. The starting and end points are green and blue dots, and the path of traversal is a red, gradient line. On all surfaces, 1ML interacts with the environment significantly more than the baseline 0ML, resulting in greater overall movement. On every surface except for compact sand, 2ML outperforms 0ML. On concrete and compact sand, 2ML had the lowest standard deviation and on the forest floor, 1ML had the lowest standard deviation. This indicates the

addition of microspine arrays also increasing the consistency and repeatability of planar locomotion with SoRos.

## V. CONCLUSION AND FUTURE WORK

SoRos have shown immense potential with inherent conformability and adaptability to a multitude of surfaces, yet they previously lacked adequate grip stability to overcome non-uniform surfaces present outside of lab environments. Compliant microspines are one missing piece towards shrinking this real-life realization gap. We propose an elegant, compliant microspine design with a standardized soft-compliant integration technique. The stacked array configuration enables the SoRo to maintain surface interaction when extreme surface discrepancies are present. We provide results from a set of field experiments reflecting the improved performance of two microspine array configurations over a baseline SoRo on four different, ruggedized surfaces. Our results indicate that microspines are a vital technology for increasing terrain traversability in mobile SoRos. Future work includes optimizing microspine array configurations for different surfaces, performing additional field experiments, and exploring the generalizability of the design to different prototypes.

## ACKNOWLEDGMENT

We thank Bek Ervin for fabricating the 0ML prototype.

## REFERENCES

- [1] B. Liu, Y. Ozkan-Aydin, D. I. Goldman, and F. L. Hammond, "Kirigami Skin Improves Soft Earthworm Robot Anchoring and Locomotion Under Cohesive Soil," in *2019 2nd IEEE International Conference on Soft Robotics (RoboSoft)*. Seoul, Korea (South): IEEE, Apr. 2019, pp. 828–833.
- [2] J. C. McKenna, D. J. Anhalt, F. M. Bronson, H. B. Brown, M. Schwerin, E. Shammas, and H. Choset, "Toroidal skin drive for snake robot locomotion," in *2008 IEEE International Conference on Robotics and Automation*. Pasadena, CA, USA: IEEE, May 2008, pp. 1150–1155.
- [3] T. G. Chen, A. Cauligi, S. A. Suresh, M. Pavone, and M. R. Cutkosky, "Testing Gecko-Inspired Adhesives With Astrobee Aboard the International Space Station: Readying the Technology for Space," *IEEE Robotics & Automation Magazine*, vol. 29, no. 3, pp. 24–33, Sep. 2022.
- [4] A. Hajj-Ahmad, L. Kaul, C. Matl, and M. Cutkosky, "GRASP: Grocery Robot's Adhesion and Suction Picker," *IEEE Robotics and Automation Letters*, vol. 8, no. 10, pp. 6419–6426, Oct. 2023.
- [5] Q. Han, A. Ji, N. Jiang, J. Hu, and S. N. Gorb, "A climbing robot with paired claws inspired by gecko locomotion," *Robotica*, vol. 40, no. 10, pp. 3686–3698, Oct. 2022, publisher: Cambridge University Press.
- [6] Sangbae Kim, M. Spenko, S. Trujillo, B. Heyneman, D. Santos, and M. Cutkosky, "Smooth Vertical Surface Climbing With Directional Adhesion," *IEEE Transactions on Robotics*, vol. 24, no. 1, pp. 65–74, Feb. 2008.
- [7] S. Sikdar, M. H. Rahman, A. Siddaiah, and P. L. Menezes, "Gecko-Inspired Adhesive Mechanisms and Adhesives for Robots—A Review," *Robotics*, vol. 11, no. 6, p. 143, Dec. 2022, number: 6 Publisher: Multidisciplinary Digital Publishing Institute.
- [8] Z. Dai, S. N. Gorb, and U. Schwarz, "Roughness-dependent friction force of the tarsal claw system in the beetle *Pachnoda marginata* (Coleoptera, Scarabaeidae)," *Journal of Experimental Biology*, vol. 205, no. 16, pp. 2479–2488, Aug. 2002.
- [9] A. T. Asbeck, S. Kim, M. R. Cutkosky, W. R. Provancher, and M. Lanzetta, "Scaling Hard Vertical Surfaces with Compliant Microspine Arrays," *The International Journal of Robotics Research*, vol. 25, no. 12, pp. 1165–1179, Dec. 2006, publisher: SAGE Publications Ltd STM.
- [10] A. T. Asbeck and M. R. Cutkosky, "Designing Compliant Spine Mechanisms for Climbing," *Journal of Mechanisms and Robotics*, vol. 4, no. 3, p. 031007, Aug. 2012.
- [11] S. Iacoponi, M. Calisti, and C. Laschi, "Simulation and Analysis of Microspines Interlocking Behavior on Rocky Surfaces: An In-Depth Study of the Isolated Spine," *Journal of Mechanisms and Robotics*, vol. 12, no. 061016, Jul. 2020.
- [12] S. Wang, H. Jiang, and M. R. Cutkosky, "Design and modeling of linearly-constrained compliant spines for human-scale locomotion on rocky surfaces," *The International Journal of Robotics Research*, vol. 36, no. 9, pp. 985–999, Aug. 2017, publisher: SAGE Publications Ltd STM.
- [13] —, "A palm for a rock climbing robot based on dense arrays of micro-spines," in *2016 IEEE/RSJ International Conference on Intelligent Robots and Systems (IROS)*. Daejeon, South Korea: IEEE, Oct. 2016, pp. 52–59.
- [14] H. Jiang, S. Wang, and M. R. Cutkosky, "Stochastic models of compliant spine arrays for rough surface grasping," *The International Journal of Robotics Research*, vol. 37, no. 7, pp. 669–687, Jun. 2018, publisher: SAGE Publications Ltd STM.
- [15] Sangbae Kim, A. Asbeck, M. Cutkosky, and W. Provancher, "SpinybotII: climbing hard walls with compliant microspines," in *ICAR '05. Proceedings., 12th International Conference on Advanced Robotics, 2005*. Seattle, WA, USA: IEEE, 2005, pp. 601–606.
- [16] S. Wang, H. Jiang, T. Myung Huh, D. Sun, W. Ruotolo, M. Miller, W. R. T. Roderick, H. S. Stuart, and M. R. Cutkosky, "SpinyHand: Contact Load Sharing for a Human-Scale Climbing Robot," *Journal of Mechanisms and Robotics*, vol. 11, no. 031009, Apr. 2019.
- [17] P. Zi, K. Xu, Y. Tian, and X. Ding, "A mechanical adhesive gripper inspired by beetle claw for a rock climbing robot," *Mechanism and Machine Theory*, vol. 181, p. 105168, Mar. 2023.
- [18] A. T. Asbeck, S. Kim, A. McClung, A. Parness, and M. R. Cutkosky, "Climbing Walls with Microspines."
- [19] Y. Liu, S. Liu, L. Wang, X. Wu, Y. Li, and T. Mei, "A Novel Tracked Wall-Climbing Robot with Bio-inspired Spine Feet," in *Intelligent Robotics and Applications*, ser. Lecture Notes in Computer Science, H. Yu, J. Liu, L. Liu, Z. Ju, Y. Liu, and D. Zhou, Eds. Cham: Springer International Publishing, 2019, pp. 84–96.
- [20] X. Li, H. Cao, S. Feng, and C. Xie, "Structure Design and Mobility Analysis of a Climbing Robot," *Journal of Physics: Conference Series*, vol. 1550, no. 2, p. 022015, May 2020, publisher: IOP Publishing.
- [21] M. Martone, C. Pavlov, A. Zeloof, V. Bahl, and A. M. Johnson, "Enhancing the Vertical Mobility of a Robot Hexapod Using Microspines," Sep. 2019, arXiv:1906.04811 [cs].
- [22] W. Ruotolo, F. S. Roig, and M. R. Cutkosky, "Load-Sharing in Soft and Spiny Paws for a Large Climbing Robot," *IEEE Robotics and Automation Letters*, vol. 4, no. 2, pp. 1439–1446, Apr. 2019.
- [23] F. Xu, J. Shen, J. Hu, and G. Jiang, "A rough concrete wall-climbing robot based on grasping claws: Mechanical design, analysis and laboratory experiments," *International Journal of Advanced Robotic Systems*, vol. 13, no. 5, p. 1729881416666777, Sep. 2016, publisher: SAGE Publications.
- [24] A. Parness, M. Frost, N. Thatte, J. P. King, K. Witkoe, M. Nevarez, M. Garrett, H. Aghazarian, and B. Kennedy, "Gravity-independent Rock-climbing Robot and a Sample Acquisition Tool with Microspine Grippers: Microspine Rock Climbing Robot," *Journal of Field Robotics*, vol. 30, no. 6, pp. 897–915, Nov. 2013.
- [25] A. Parness, N. Abcouwer, C. Fuller, N. Wiltsie, J. Nash, and B. Kennedy, "LEMUR 3: A limbed climbing robot for extreme terrain mobility in space," in *2017 IEEE International Conference on Robotics and Automation (ICRA)*. Singapore, Singapore: IEEE, May 2017, pp. 5467–5473.
- [26] A. Parness, T. Evans, W. Raff, J. King, K. Carpenter, A. Willig, J. Grimes-York, A. Berg, E. Fouad, and N. Wiltsie, "Maturing Microspine Grippers for Space Applications through Test Campaigns," in *AIAA SPACE and Astronautics Forum and Exposition*. Orlando, FL: American Institute of Aeronautics and Astronautics, Sep. 2017.
- [27] T. D. Ta, T. Umedachi, and Y. Kawahara, "Design of Frictional 2D-Anisotropy Surface for Wriggle Locomotion of Printable Soft-Bodied Robots," in *2018 IEEE International Conference on Robotics and Automation (ICRA)*. Brisbane, QLD: IEEE, May 2018, pp. 6779–6785.
- [28] X. Yang, R. Tan, H. Lu, and Y. Shen, "Starfish Inspired Milli Soft Robot With Omnidirectional Adaptive Locomotion Ability," *IEEE Robotics and Automation Letters*, vol. 6, no. 2, pp. 3325–3332, Apr. 2021.
- [29] Q. Hu, E. Dong, G. Cheng, H. Jin, J. Yang, and D. Sun, "Inchworm-inspired soft climbing robot using microspine arrays," in *2019 IEEE/RSJ International Conference on Intelligent Robots and Systems (IROS)*. Macau, China: IEEE, Nov. 2019, pp. 5800–5805.
- [30] K. A. Daltorio, T. E. Wei, A. D. Horchler, L. Southard, G. D. Wile, R. D. Quinn, S. N. Gorb, and R. E. Ritzmann, "Mini-whigs tm climbs steep surfaces using insect-inspired attachment mechanisms," *The International Journal of Robotics Research*, vol. 28, no. 2, p. 285–302, Feb. 2009. [Online]. Available: <https://journals.sagepub.com/doi/10.1177/0278364908095334>
- [31] M. J. Spenko, G. C. Haynes, J. A. Saunders, M. R. Cutkosky, A. A. Rizzi, R. J. Full, and D. E. Koditschek, "Biologically inspired climbing with a hexapodal robot," *Journal of Field Robotics*, vol. 25, no. 4–5, p. 223–242, Apr. 2008. [Online]. Available: <https://onlinelibrary.wiley.com/doi/10.1002/rob.20238>
- [32] C. Freeman, M. Maynard, and V. Vikas, "Topology and Morphology Design of Spherically Reconfigurable Homogeneous Modular Soft Robots," *Soft Robotics*, vol. 10, no. 1, pp. 52–65, Feb. 2023, publisher: Mary Ann Liebert, Inc., publishers.
- [33] C. Freeman, A. N. Mahendran, and V. Vikas, "Environment-centric learning approach for gait synthesis in terrestrial soft robots," 2024. [Online]. Available: <https://arxiv.org/abs/2402.03617>
- [34] E. Olson, "Apriltag: A robust and flexible visual fiducial system," in *2011 IEEE International Conference on Robotics and Automation*, May 2011, p. 3400–3407. [Online]. Available: <https://ieeexplore.ieee.org/document/5979561>